Heloisa P. Macedo, Rodolfo L.B.A. Medeiros, Jan Ilsemann, Dulce M.A. Melo, Kurosch Rezwan, Michaela Wilhelm

Nickel-containing hybrid ceramics derived from polysiloxanes with hierarchical porosity for CO2 methanation

Recommended Citation (primary publication/Version of Record) incl. DOI:

Heloisa P. Macedo, Rodolfo L.B.A. Medeiros, Jan Ilsemann, Dulce M.A. Melo, Kurosch Rezwan, Michaela Wilhelm, Nickel-containing hybrid ceramics derived from polysiloxanes with hierarchical porosity for CO2 methanation, Microporous and Mesoporous Materials, Volume 278, 2019, Pages 156-166, ISSN 1387-1811, https://doi.org/10.1016/j.micromeso.2018.11.006

Nickel-containing hybrid ceramics derived from polysiloxanes with hierarchical porosity for CO_2 methanation

Heloisa P. Macedo[a,b], Rodolfo L.B.A. Medeiros[b], Jan Ilsemann[c], Dulce M.A. Melo[b], Kurosch Rezwan[a,d], Michaela Wilhelm[a,*]

[a] Advanced Ceramics, University of Bremen, Bremen, Germany
[b] Post-Graduate Program in Materials Science and Engineering, Federal University of Rio Grande do Norte, Natal, RN, Brazil
[c] Institute of Applied and Physical Chemistry, University of Bremen, Bremen, Germany
[d] MAPEX, Center for Materials and Processes, University of Bremen, Germany

ARTICLE INFO

Keywords:
Hybrid ceramics
Polysiloxane
Polymer-derived ceramic
Complexing agent
Nickel catalyst
CO_2 methanation

ABSTRACT

Nickel-containing hybrid ceramics were prepared by pyrolytic conversion from either methyl or methyl-phenyl polysiloxanes mixed with bistrimethoxysilylpropylamine (BisA) as a complexing agent and nickel salt. Materials with tailorable characteristics were generated by varying the pyrolysis temperature from 400 up to 600 °C in order to evaluate their applicability in the CO_2 methanation. The materials were characterized by thermogravimetric analysis (TGA), N_2 adsorption-desorption isotherms (BET-BJH), water and *n*-heptane adsorption, X-ray diffraction (XRD) and transmission electron microscopy (TEM). In-situ X-ray diffraction analysis (in-situ XRD) was used to evaluate the Ni particle structure and size during a simulated catalytic reaction. Porous hybrid ceramics (ceramers) with high specific surface areas (100–550 $m^2 g^{-1}$), hydrophobic or hydrophilic surfaces and different Ni particle sizes (4–7 nm) were obtained by varying the pyrolysis temperature and polysiloxane composition. The pyrolytic conversion of polysiloxanes combined with the complexing amino-siloxane BisA not only permitted a good dispersion of the Ni nanoparticles but also enabled the formation of hierarchical porosity with micro-, meso- and macropores. Regarding the catalytic performance, ceramers prepared from methyl polysiloxane exhibited a more hydrophobic surface and improved catalytic performance compared to the ones prepared from methyl-phenyl polysiloxane. A negative effect on the catalytic performance of ceramers was observed with increasing pyrolysis temperatures, which led to an increase in Ni particle size (from 4 to 7 nm), and lower levels of conversion and selectivity. The ceramers pyrolyzed at 400 °C exhibited the best catalytic performance, showing selectivity up to ~77% and good stability over a 10 h test, during which the Ni particle size was preserved.

1. Introduction

Preceramic polymers such as polysiloxanes, polycarbosilanes or polysilazanes are organosilicon polymers that can be converted to ceramic through pyrolysis under inert atmospheres [1]. Such materials, known as Polymer-Derived Ceramics (PDCs), are Si-based advanced ceramics that have attracted great attention over the past years due to their low-cost synthesis, simple processing methodology and large range of properties such as high thermal and chemical stability, outstanding oxidation and corrosion resistance, low density, high permeability and good mechanical strength [2,3]. The pyrolytic conversion of polymeric siloxanes at temperatures of 400–1500 °C can be used to adjust the ceramic characteristics, resulting in interesting physicochemical properties. Pyrolysis between 400 and 800 °C, for instance, leads to porous and surface-rich materials, so-called ceramers, in a hybrid state where the polymer is just partly converted to ceramic [4]. The well-controlled pyrolytic conversion at intermediate temperatures is decisive to change the nature of the surface hydrophobicity and to develop micro- and mesopores leading to components with high porosity [5].

Due to their unique properties, PDCs have been studied for various engineering applications such as sensors [6], fibers [7], anodes [8], coatings [9] and membranes [10]. A relatively new potential use for these materials is the application of metal-containing PDCs for heterogeneous catalytic reactions. Over the past years, few studies have reported the preparation of nickel, iron, cobalt, palladium, and

* Corresponding author.
E-mail address: mwilhelm@uni-bremen.de (M. Wilhelm).

https://doi.org/10.1016/j.micromeso.2018.11.006
Received 17 August 2018; Received in revised form 1 November 2018; Accepted 4 November 2018
Available online 06 November 2018
1387-1811/

platinum-containing PDCs for different catalytic applications [11–17]. In earlier studies of our group, porous ceramers derived from polysiloxanes with well-distributed metal nanoparticles (Ni, Pt, Co) showed improved catalytic performance for CO oxidation, CO_2 methanation and Fischer-Tropsch reactions [18–22]. It was demonstrated that by using an amine-containing siloxane as a complexing precursor, the metal particles could be stabilized, preventing them from sintering and agglomeration.

Catalytic hydrogenation of CO_2 to methane, also called Sabatier reaction ($CO_2 + 4H_2 \rightarrow CH_4 + 2H_2O$, $\Delta H^0 = -164\,kJ\,mol^{-1}$) has attracted attention over the last decades by converting greenhouse gases such as CO or CO_2 into a valuable-added gas (CH_4). Methane can be used as a fuel, being directly fed to the gas grid or stored in tanks, and as raw material for the production of other chemicals [23]. The reduction of carbon dioxide to methane is an eight-electron process with significant kinetic barriers, which thus, requires a highly active catalyst to achieve acceptable rate and selectivity [24].

Noble (Rh, Ru and Pd) and transition (Ni, Fe and Co) metal-based catalysts are the most investigated catalysts for the CO_2 methanation [25–30]. Nobel metals are known to be very active at low temperatures, however, Ni-based catalysts are most commonly employed and promising for industrial applications, owing to the low-cost, abundance and high activity [31]. As pointed out by Le et al. [32] a high Ni dispersion and strong CO_2 adsorption can improve the catalytic activity for CO_2 methanation. In general, the metal species tend to be highly dispersed on the support at low metal loadings, whereas the metal particles tend to aggregate at high metal loadings [33]. According to Yan et al. [34] catalysts with moderate Ni-support interaction showed superior activity for CO_2 methanation, whereas inferior activity was obtained with an overly strong metal-support interaction.

The support plays an important role in the performance of a heterogeneous catalyst, with the major role to disperse the active component. It usually affects the morphology of the active phase, adsorption capability, metal-support interaction and catalytic properties [35,36]. Supports with high specific surface areas, usually oxides as SiO_2 [37] and Al_2O_3 [38], have been extensively studied for the preparation of well-dispersed catalysts. Besides, since water is formed as a product during methanation reaction, a hydrophobic support is favorable to avoid the blocking of the adsorption sites. Moreover, the preparation methodology has a significant effect on the catalytic performance, influencing the metal-support interaction as well as the dispersion of the active metal [39,40]. In order to improve the efficiency of the catalyst, it is important to ensure highly dispersed and easily accessible nanoparticles. Various methods have been investigated for preparing the catalysts including impregnation, co-precipitation, sol-gel, hydrothermal and combustion method [41–44].

One advantage of the PDC route, in comparison to the conventional preparation methods, is the in-situ reduction of the metal during the pyrolysis [45], by which the formation of hardly reducible mixed oxides can be avoided. As the particles are already in the metallic state only an activation step is required prior to the reaction. Furthermore, the properties such as porosity, surface hydrophobicity and metal dispersion can be easily adjusted by varying the pyrolysis temperature and precursor composition [5].

The present study focuses on the preparation of highly porous and well-dispersed Ni-containing hybrid ceramics derived from polysiloxanes and their applicability as catalyst in the CO_2 methanation reaction. Our goal is by adding bistrimethoxysilylpropylamine (BisA) as a complexing agent to disperse the metal particles in the polysiloxane matrix, and in particular, induce the generation of mesopores in order to facilitate the mass transfer inside the catalyst. The influence of the pyrolysis temperature (400–600 °C) and polysiloxane precursor (with either methyl or methyl-phenyl groups) on the material properties and catalytic activity is investigated.

2. Materials and methods

2.1. Preparation

All chemicals used in the present study were of analytical grade and used as received without further purification. The synthesis procedure carried out is similar to previous works [21,22]. Two types of ceramers were prepared using different polysiloxane precursors such as methylphenyl polysiloxane (Silres® H44, Wacker Chemie AG) or methyl polysiloxane (Silres® MK, Wacker Chemie AG). Using BisA (Bistrimethoxysilylpropylamine, abcr GmbH) as a complexing agent, a molar ratio of nickel to the complexing siloxane was fixed at 1:4, to ensure the complete complexation of the metal ions. First, the nickel (II) nitrate hexahydrate (Merck KGaA), the polysiloxane precursor (H44 or MK) and the complexing agent BisA were separately dissolved in THF (tetrahydrofuran, Fisher Scientific). Afterwards, these solutions were slowly mixed together and then a 0.2-M-NH_3-solution was added as a catalyst for the hydrolysis-condensation reactions. The whole solution was stirred at 85 °C for 72 h. After the solvent removal, the samples were cross-linked at 200 °C for 2 h. The materials were pyrolyzed at 400, 500 or 600 °C under N_2-atmosphere. The heating rate for the pyrolysis process was 120 °C h^{-1} to 100 °C below the final temperature and 30 °C h^{-1} to reach the maximum temperature with a dwelling time of 4 h. Ceramers with ~5 wt% of Ni after pyrolysis were prepared for both polysiloxanes precursors. Furthermore, nickel-free samples were also produced using a molar ratio of polysiloxane to BisA of 1:0.4. The preparation route and precursors used are shown in Fig. S1 in supplementary data. The calculated amounts are given in Table 1, including the samples nomenclature. The endings of the name denote the pyrolysis temperature. For comparison of catalytic performance, a standard catalyst with 5 wt% of Ni was prepared by wet impregnation of nickel (II) nitrate hexahydrate (Merck KGaA) on a commercial fumed silica support (Aerosil-380, Evonik Industries AG), followed by drying at 70 °C for 12 h and pyrolysis at 400 °C using the same conditions as described above. The characterization results for this catalyst, named Ni/SiO_2-400, can be found in the supplementary data as well.

2.2. Characterization

The decomposition and thermal behavior of the cross-linked ceramers were analyzed by thermogravimetric analysis in a STA 503 thermal analysis system from BÄHR Thermoanalyse GmbH up to 1000 °C with a heating rate of 2 °C min^{-1} and a flow rate of 2 L h^{-1} of

Table 1
Prepared materials and their composition, pyrolysis temperature and Ni content.

Sample	Polysiloxane precursor	Ratio (mol) Polysiloxane:BisA:Ni	Pyrolysis temperature (°C)	Ni content (wt%) after pyrolysis
H44 + BisA-xxx	H44	1:0.4:0	400/500/600	–
MK + BisA-xxx	MK	1:0.4:0	400/500/600	–
Ni/H44 + BisA-xxx	H44	1:1.2:0.3[a]	400/500/600	4.41[b]/4.81[c]/5.01[d]
Ni/MK + BisA-xxx	MK	1:1.2:0.3[a]	400/500/600	5.08[b]/5.36[c]/5.51[d]

[a] Ni/BisA molar ratio: 1:4.
[b], [c], [d] Calculated from TGA at 400, 500 and 600 °C, respectively (dwell time of 4 h).

N_2. In order to calculate the metal content, firstly, the amount of inserted metal was calculated from the amount of metal salt added. Then, the metal content could be calculated by determining the weight loss during pyrolytic conversion. The specific surface area, pore volume, and pore size distributions were determined by nitrogen adsorption-desorption isotherms at relative pressures P/P_0 of 0.1–0.99 at 77 K (Belsorp-Mini, Bel Japan, Inc.). Surface areas were calculated from adsorption data using the BET method at P/P_0 ranging from 0.1 to 0.3, while pore volume and pore size were determined from the desorption data by the BJH method. Previously, the samples were outgassed for 12 h at 120 °C under vacuum. The surface characteristics (hydrophilicity and hydrophobicity) were investigated by water and *n*-heptane vapor adsorption measurements. First, ~0.5 g of samples (particle sizes ≤300 μm) were dried at 70 °C for 24 h and then stored inside closed Erlenmeyer flasks at room temperature under *n*-heptane or water vapor atmosphere. After 24 h the weight of the samples was measured and the amount of adsorbate was determined. The crystalline structure and average crystallite size of Ni were determined for the Ni-containing samples by X-ray diffraction in a Shimadzu XRD 7000 apparatus using Cu-Kα radiation (1.5409 Å), 2θ ranging from 10° to 80° in steps of 0.02° and a counting time per step of 2° min^{-1}. The crystallite size was calculated from the most intense peak (111) using Scherrer's equation [46]. TEM images were acquired using a FEI Titan 80/300 microscope coupled with an imaging filter operating at 300 keV voltage. The samples were analyzed after different pyrolysis temperatures to determine the metal distribution and particle size, which were calculated based on 100 particles for each image and then statistically analyzed.

2.3. Catalytic tests and in-situ analysis

A tubular fixed-bed reactor was used to carry out the catalytic tests at atmospheric pressure in order to compare the activity and selectivity of each sample. Therefore, 50 mg of the powder catalyst (sieve fraction of 100–200 μm) and 300 mg of Al_2O_3 were fixated with quartz wool in a quartz-glass tube reactor (inner diameter of 6 mm). The total flow rate was set at 50 mL_N min^{-1} composed of $H_2/CO_2/Ar$ = 4/1/5, which gives a weight hourly space velocity (WHSV) of 60 L g_{cat}^{-1} h^{-1}. The catalysts were tested between 200 and 400 °C in intervals of 50 °C. Each temperature was held for 42 minutes and the outflowing gas was continuously monitored with an on-line compact gas chromatograph (Global Analyser Solution) equipped with a thermal conductivity detector. Two columns were used, a RT-Molsieve 5 Å column (15 m) to detect CO and CH_4, and a RT-Porabond column (30 m) for the detection of CO_2. The CO_2 conversion, as well as CH_4 yield and selectivity, were determined according to the following equations:

$$X_{CO_2} = 1 - \frac{c_{CO_2,out}}{c_{CO_2,out} + c_{CH4,out} + c_{CO,out}} \quad (1)$$

$$Y_{CH_4} = \frac{c_{CH_4,out}}{c_{CO_2,out} + c_{CH_4,out} + c_{CO,out}} \quad (2)$$

$$S_{CH_4} = \frac{Y_{CH_4}}{X_{CO_2}} \quad (3)$$

In pre-experiments, no higher hydrocarbons were found. The catalysts were activated in-situ by flowing H_2 at 430 °C for 10 h (heating ramp 1 °C/min). Afterwards, the reactor was cooled down in inert gas atmosphere. All tubing was heated to prevent water from condensing in the experimental set-up.

The *in-situ* X-ray diffraction analysis (*in-situ* XRD) was performed to evaluate the nickel crystallite size during a simulated CO_2 methanation reaction at 400 °C for 1 h. The measurement was performed on a XPD-10B beamline from the Brazilian Synchrotron Light Laboratory - LNLS. The samples were placed in a furnace installed in the goniometer (Hubber model) operating in Bragg-Brentano geometry (θ-2θ) and equipped with a Mythen-1 K detector (Detris) located on a meter of the oven. Scans were performed in the 2θ range from 35 to 65° to verify the formation of the main peaks, using a radiation with a wavelength of 1.7712 Å and energy of 7000 eV. The crystallite size was calculated from the Scherrer's equation [46] based on the main peak (111). The experiment was conducted under the following conditions: (i) activation using a mixture of 5% H_2/He with a flow rate of 75 ml min^{-1} at 430 °C for 1 h; (ii) cool down to 400 °C while purging with He for 30 min; and (iii) start of reaction by flowing a mixture of 40% of H_2, 10% of CO_2 and 50% of He (total flow rate of 50 ml min^{-1}) at 400 °C for 1 h.

3. Results and discussions

3.1. Pyrolytic conversion

The high thermal stability of polysiloxanes is one of the most important properties of this class of polymers and is directly related to the high energy and ionic character of the Si-O bond. The thermal degradation happens mainly through the cleavage and reorganization of the organic groups and several bonds (Si-CH_3, Si-C_6H_5, Si-H, Si-CH_2-Si, etc), which yields a mixture of volatile compounds and free (hydro) carbon, resulting in a weight loss [47,48]. The decomposition behavior of the cross-linked polysiloxanes and the ceramers was investigated by thermogravimetric analysis up to 1000 °C as shown in Fig. 1. At temperatures below 400 °C the evaporation of mainly cross-linked products (water and alcohols), oligomers and solvent are observed, which are released while the cross-linking of siloxanes is accomplished [49]. At higher temperatures (~450–800 °C) the decomposition of the organic groups takes place by breaking Si-H, Si-C and C-H bonds with the release of typical hydrocarbons, CH_4, H_2 or other volatile compounds. At temperatures beyond 800 °C mainly H_2 is eliminated [50]. Regarding the pure commercially available polysiloxanes H44 and MK, a higher overall thermal stability is observed for MK. The onset of significant decomposition of H44 and MK starts around 500 °C and 600 °C, respectively, with H44 presenting a higher weight loss at 1000 °C (~24%) compared to MK (~17%). Phenyl groups have a higher carbon content and, although more carbon will remain in the structure, the overall weight loss for H44 is higher. The residue after pyrolysis for H44 corresponds to the atomic proportions of 18.7% Si–28.7% O–52.6% C, while that for MK is 31.6% Si–48.1% O–20.2% C [49]. This could be explained by the higher decomposition of the phenyl groups present in H44 as well to a decrease in molecular weight and increased loss of small oligomers formed by depolymerization [50].

For the metal-free ceramers (H44 + BisA and MK + BisA), the decomposition starts at lower temperatures, approximately at 400 °C,

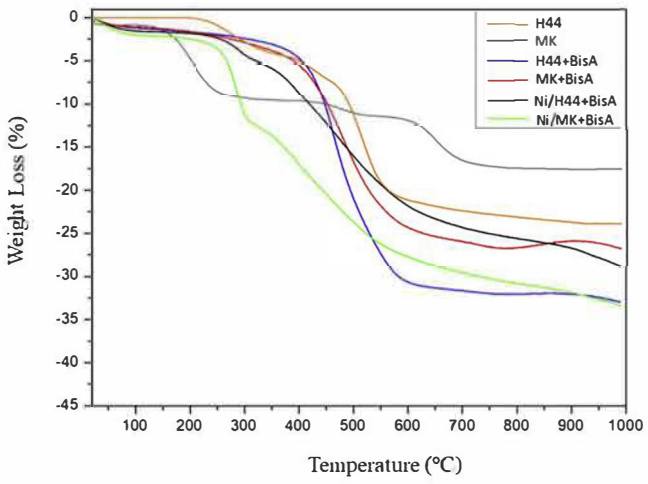

Fig. 1. Thermogravimetric analysis of cross-linked precursors under N_2 atmosphere.

characterized by a strong weight loss. This indicates a reduced thermal stability of the aminopropyl groups from the complexing agent compared to the organic groups of the polysiloxanes. At about 600 °C the weight loss levels off, indicating that the majority of the polymer-to-ceramic conversion has occurred. Ceramers prepared from a methyl polysiloxane (MK) presented higher ceramic yield when compared to the ones prepared with methyl-phenyl polysiloxane (H44).

By adding nickel, the decomposition during the pyrolytic conversion is slightly shifted to lower temperatures indicating that nickel catalyzes the decomposition process to a certain extent. After the initial weight loss, the decomposition continues with increasing the temperature. The overall weight loss for the Ni-containing ceramers is about 15–23% at 400 °C and increases to 25–30% at 600 °C, resulting in a slightly higher Ni content (wt%) at 600 °C, as seen in Table 1. This behavior has been also observed for polysiloxanes containing others metal as reported in the literature [19–21].

Therefore, the thermal stability and decomposition behavior are intrinsically influenced by the pyrolysis temperature, composition of the polysiloxane, and presence of the complexing agent and metal precursor.

3.2. Porosity

For catalytic applications, a high specific surface area material with hierarchical porosity is desired to improve the dispersion of the active phase and to facilitate internal mass transfer, leading to increased catalytic activity. The porosity in polymer-derived ceramics can be further engineered by developing micro- and mesopores through a controlled pyrolytic treatment as a result of the decomposition of organic groups and release of volatiles. N_2-adsorption/desorption isotherms were measured to evaluate the pore structure and the specific surface area (SSA). Fig. 2(a) shows the obtained N_2-isotherms. The corresponding BJH plots, illustrating the respective pore size distribution, are shown in Fig. 2(b).

The results show isotherms which are in an intermediate state of type II behavior, but also partly of type IV, which are typical for macro- and mesoporous materials, respectively [51]. Additionally, a considerable amount of micropores is expected as indicated by the significant adsorption at relatively lower pressures (p/p_0). Therefore, the ceramers show a hierarchical porosity formed by micro-, meso- and macropores, which is of great importance for many applications such as catalysis and adsorption [52].

The pure polysiloxanes H44 and MK present isotherms of type I after pyrolysis (not shown), which is related to the predominant presence of micropores. By adding BisA, meso- and macropores are further generated for both metal-free and Ni-containing ceramers, revealing the same overall trend at temperatures of 400–600 °C. Furthermore, cross-linked samples also show meso- and macropores as evidenced by the isotherms and pore size distributions (see Fig. S2 in supplementary data), indicating that the addition of BisA induces the evolution of meso- and macroporosity even before pyrolysis. Considering that the nickel ions

Table 2
Average pore size, average pore volume, Ni average crystallite and particle size from ceramers pyrolyzed at 400, 500 and 600 °C.

Sample	Average pore size (nm)[a]	Average pore volume ($cm^3\ g^{-1}$)[a]	Ni average crystallite size (nm)[b]	Ni average particle size (nm)[c]
H44 + BisA-400	3.75	0.1792	–	–
H44 + BisA-500	3.75	0.5365	–	–
H44 + BisA-600	3.75	0.1951	–	–
MK + BisA-400	9.23	0.8374	–	–
MK + BisA-500	9.23	0.9428	–	–
MK + BisA-600	9.23	0.8019	–	–
Ni/H44 + BisA-400	5.46	0.4580	4.9	4.3
Ni/H44 + BisA-500	5.46	0.5959	7.8	–
Ni/H44 + BisA-600	5.46	0.4081	13.5	7.3
Ni/MK + BisA-400	18.37	0.9479	4.3	4.0
Ni/MK + BisA-500	18.37	1.1411	7.6	–
Ni/MK + BisA-600	18.37	1.1240	11.5	7.0

[a] Calculated by the BJH method from N_2-desorption.
[b] Calculated from XRD based on Scherrer's equation.
[c] Calculated from TEM images based on 100 particles for materials pyrolyzed at 400 and 600 °C.

are surrounded primarily by the complexing siloxane chains and that an increased decomposition is observed when BisA is present, the formation of a higher porosity directly around the nickel can be expected, what explains the development of larger pores and improved metal accessibility with the presence of the complexing siloxane. Prenzel et al. [53] also prepared ceramers with mesoporosity by using MK and BisA as precursors and pyrolyzing the samples at temperatures of 350–600 °C.

The hysteresis can be correlated with a type H3 found for materials with aggregates of plate-like particles giving rise to slit-shaped pores [54]. For ceramers prepared with methyl polysiloxane (MK + BisA and Ni/MK + BisA), the adsorption strongly increased in the range of $p/p_0 \sim 1$, indicating a higher pore volume with the presence of bigger pores as confirmed by the pore size distributions (Fig. 2(b)). The addition of Ni led to an increase in pore size and pore volume as shown in Table 2 for both types of ceramers. This could be caused by an enhanced decomposition of the siloxanes around the Ni nanoparticles. Broader pore size distribution was observed for Ni/MK + BisA ceramers with bigger pores up to 90 nm, an average pore size of 18.37 nm and pore volume up to of 1.1 $cm^3\ g^{-1}$ (see Table 2). On the other hand, a narrow distribution was observed for Ni/H44 + BisA ceramers consisting of pores up to 35 nm, an average pore size of 5.46 nm and pore volume up to 0.59 $cm^3\ g^{-1}$. Regarding the metal-free ceramers, MK + BisA materials presented larger pore sizes and pore volumes compared to H44 + BisA ceramers, both revealing narrow distributions. The BJH results for the metal-free and Ni-containing ceramers pyrolyzed at temperatures of 400–600 °C confirm the presence of mesoporous. The average pore size was not affected by the increased temperature, however, the pore volume increased from 400 to 500 °C, and decreased from 500 to 600 °C,

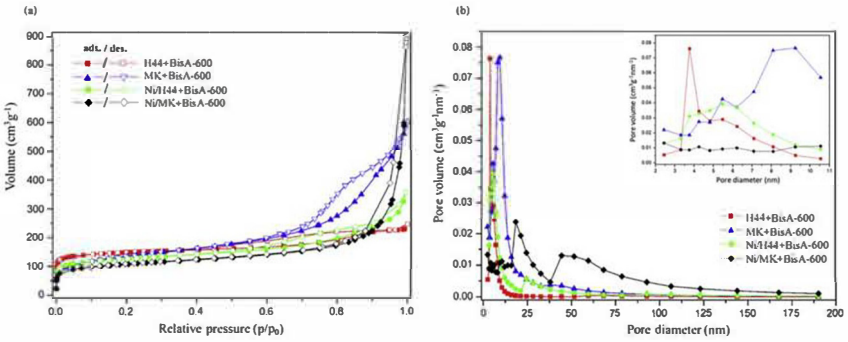

Fig. 2. (a) N_2-adsorption/desorption isotherms and (b) pore size distribution (inset from 2 to 11 nm) of ceramers pyrolyzed at 600 °C.

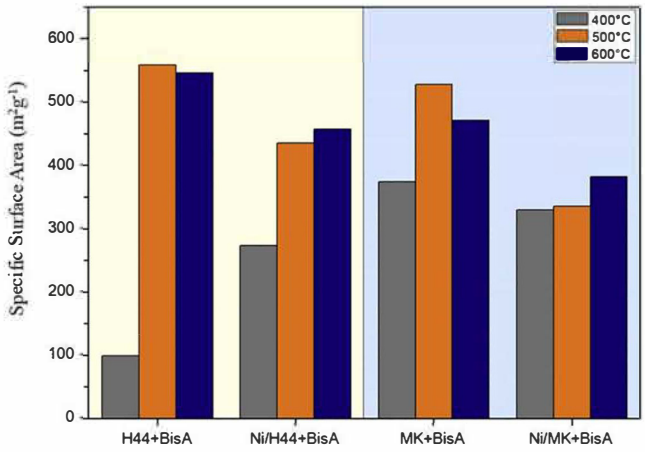

Fig. 3. Specific BET surface areas of metal-free and Ni-containing ceramers pyrolyzed at 400, 500 and 600 °C.

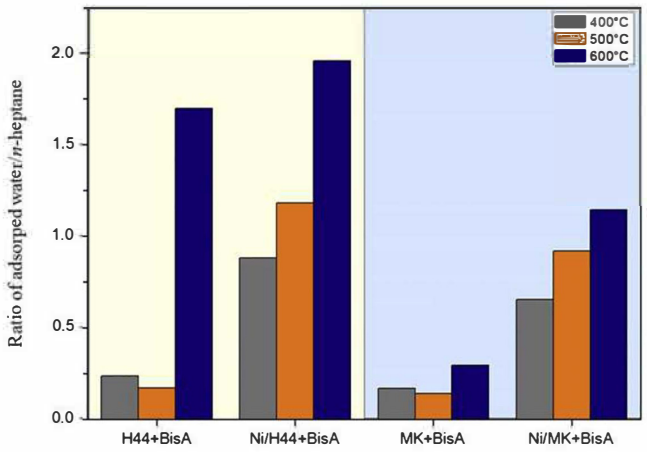

Fig. 4. Ratio of maximum water and *n*-heptane adsorption for ceramers pyrolyzed at 400, 500 and 600 °C.

following the same trend as the specific surface area (see Fig. 3).

The specific BET surface areas calculated from the nitrogen adsorption isotherms are shown in Fig. 3. Surface areas of 100–550 $m^2 g^{-1}$ and 330–530 $m^2 g^{-1}$ were generated for ceramers prepared using H44 and MK as polysiloxanes, respectively. Porosity is generated through the gases released during the polymer-to-ceramic transformation due to the decomposition of the CH_3, C_3H_6-NH_2 and C_6H_5 groups, resulting in a porous structure with high SSA. This porosity is however transient since the pores are only stable at temperatures as high as their initial pyrolysis temperature [55,56]. Comparing the metal-free samples, a dependency of the SSA over the pyrolysis temperature was observed. With increasing pyrolysis temperature from 400 °C to 500 °C the SSA increases, what can be explained by the decomposition of the organic groups, leading to the development of porosity and high SSA. The highest surface areas are detected for the metal-free samples after pyrolysis at 500 °C in the range of 500 $m^2 g^{-1}$. However, a further increase in the pyrolysis temperature leads to a decrease in the surface areas, since the pores start to collapse [57]. Regarding the Ni-containing ceramers, the same trend is observed, with increasing pyrolysis temperature the SSA increases. However, lower surface areas are observed for the ceramers pyrolyzed at 500 and 600 °C compared to the metal-free samples. This can be explained by the fact that Ni-containing ceramers show a higher density, and also by the influence of Ni on the decomposition of the precursors during pyrolysis, as observed in the thermogravimetric measurements. This behavior has also been observed for polysiloxanes containing others metal as reported in the literature [18,19,22].

Summarizing, these results demonstrate that the microstructure of the material can be tailored by varying the pyrolysis temperature, by the addition of metal salt and the polysiloxane composition. Therefore, materials with high surface area and hierarchical porosity can be generated.

3.3. Surface characteristics

In catalysis, the support plays an important role in the catalyzed reaction due to the metal-support or reactant-support interactions. Especially in reactions where water is formed as a product, a hydrophobic support is favorable to avoid the blocking of the adsorption sites by water as observed in methanation reactions [33,58] and catalyzed oxidation of volatile organic compounds [59]. Therefore, it is of great interest to investigate how the precursor composition and the pyrolysis temperatures influence the surface characteristics of the materials. Thus, the surface hydrophilicity and hydrophobicity were analyzed by water (which is mainly polar) and *n*-heptane (which shows mainly dispersive interaction [52]) adsorption measurements. The amount of *n*-heptane and water adsorbed at ambient pressure displays the maximum adsorption capacity, and the ratio of the two adsorbates gives a first (non-quantitative) idea of the degree of hydrophilicity. This method provides a simple way to obtain initial information about the hydrophobicity/hydrophilicity of porous media. The ratio of adsorbed water/*n*-heptane for all prepared ceramers is shown in Fig. 4. The values of the specific BET surface areas from Fig. 3 were used to calculate the amount of solvent adsorbed per square meter of the ceramers surface area.

The hydrophobicity can be adjusted by varying the pyrolysis temperature. At 400 °C the ceramers are strongly hydrophobic showing a predominant adsorption of *n*-heptane in contrast to the lower adsorption of water. Decomposition of the organic compounds starts at around 450 °C, converting the organic part into free (hydro)carbon, with a still hydrophobic matrix. During pyrolysis of phenyl and methyl group-containing polysiloxanes, the phenyl groups are easily converted at lower temperatures than the methyl groups. Therefore, the conversion from strongly hydrophobic to hydrophilic starts at different pyrolysis temperatures, for H44 at around 600 °C and for MK above 630 °C [5]. Thus, the metal-free and Ni-containing ceramers prepared with MK show a more hydrophobic behavior compared to the ones with H44. For the metal-free ceramers there is a low uptake of water but an increased uptake for *n*-heptane. The situation is different for the Ni-containing ceramers where the ratio of water to *n*-heptane adsorption is inverted, revealing more hydrophilic materials. Ni catalyzes the decomposition reaction of the hydrophobic organic groups, as shown in the thermogravimetric measurements, leaving behind a higher amount of inorganic parts remaining in the material. Regarding the pyrolysis temperature, with increasing the temperature a significant increase in water and decrease in *n*-heptane adsorption is found, since less hydrophobic organic groups are present due to the loss of the methyl and phenyl groups, resulting in a more hydrophilic surface. This is sustained by comparing the weight losses at 400 and 600 °C (Fig. 1) taken from the TGA profile, where the weight loss for all ceramers is about 5–17% at 400 °C and increases to 12–31% at 600 °C.

Accordingly, these results demonstrate that the surface properties are influenced by the precursor composition, by the metal addition and strongly by the pyrolysis temperature. Therefore, this preparation route is suitable for generating hydrophobic as well as hydrophilic catalytic materials.

3.4. Metallic nanoparticles

For catalytic applications, it is important to ensure highly dispersed and easily accessible nanoparticles in order to improve the utilization of the metal catalyst and increase the catalytic activity. For structure-

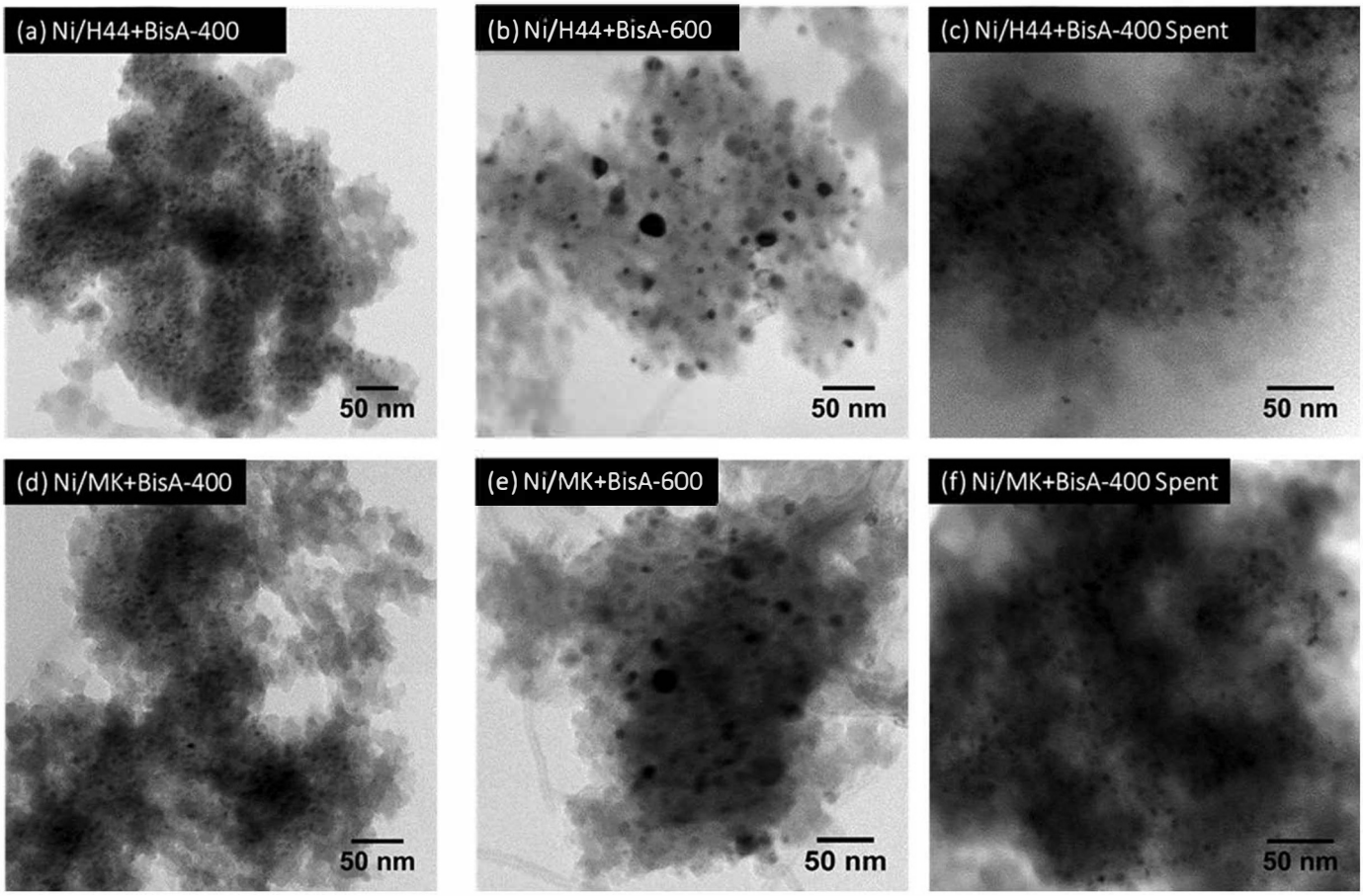

Fig. 5. TEM images of the fresh Ni-containing ceramers pyrolyzed at 400 °C (a,d), 600 °C (b,e) and the spent catalysts after a 10 h stability test (c,f).

sensitive reactions such as the CO_2 methanation, a serious problem is often the sintering of metallic particles at higher temperatures, resulting in a decrease in the activity and long-term stability of the catalyst [60]. Thus, an effective preparation of highly dispersed metal nanoparticles with low or no particle growth at the same time is of great interest. The complexing agent plays an important role during the processing route due to the complexation of the nickel ions by the amino groups. After cross-linking, the siloxane is bond to the polymer precursor, which ensures the dispersion and thermally stable embedding of the nickel particles throughout the matrix [19]. Investigations reported in the literature have indicated a more homogeneous distribution of metallic particles throughout the matrix if complexing siloxanes are incorporated as precursor [20,21].

The formation and distribution of Ni nanoparticles were investigated by TEM analysis of the fresh ceramers pyrolyzed at 400 and 600 °C, and after 10 h of reaction as shown in Fig. 5 (a–f). The particle size distributions can be found in the supplementary data (Fig. S3). The effect of the pyrolysis temperature on the size and distribution of the metal nanoparticles is clearly demonstrated. Similar Ni particle sizes and distributions are found for both types of ceramers (see Table 2). The complexing siloxane BisA seems to effectively stabilize and homogeneously disperse the nickel nanoparticles at low pyrolysis temperatures of 400 °C, resulting in an average particle size of ~4 nm. At higher pyrolysis temperature of 600 °C, a still homogeneous distribution is observed, however with the formation of bigger particles with an average size of ~7 nm. This is an unexpected result as in similar siloxane-based catalysts the use of a complexing agent with amino groups was essential for the generation of well-distributed metal nanoparticles (Ni, Pt) and for the suppression of particle clustering during varied pyrolysis temperatures [18–22].

This unforeseen result could be addressed probably due to the higher local temperature caused by the pyrolysis of a greater number of organic groups. Harms et al. [61] reported in their work the preparation of siloxane-based electrocatalysts with platinum nanoparticles (2.5–3.4 nm) homogeneously distributed on the support at pyrolysis temperature of 500 °C, whereas a higher pyrolysis temperature of 600 °C led to agglomeration of the metal particles. Complexing agent-free samples showed larger particles (4.7 nm) and agglomerates. Scheffler et al. [62] described the formation of Ni nanoparticles with average sizes around 40–60 nm after pyrolysis of Ni-containing polysiloxanes without complexing agent between 700 and 1000 °C.

In Fig. 5(c) and 5(f), images of ceramers (pyrolyzed at 400 °C) obtained after testing the samples during 10 h for the CO_2-methanation at a temperature of 350 °C are presented. No sign of sintering of the Ni particles was found, demonstrating a good stability of the ceramers, which displayed an average particle size of 4.6 and 4.3 nm for Ni/H44 + BisA and Ni/MK + BisA, respectively.

Further investigation on the Ni particles was conducted by X-ray diffraction analysis, which is depicted in Fig. 6 with the XRD patterns of the fresh Ni-containing ceramers pyrolyzed at temperatures of 400, 500 and 600 °C. The XRD patterns showed broad reflections between 15 and 30° 2θ indicating the formation of Si-based amorphous phase. Additionally, the materials presented characteristic diffraction peaks corresponding to the crystallographic planes of cubic Ni structure with Fm-3m symmetry (JCPDS No. 01-89-7128) around 45°, 52° and 77° 2θ, indicating the formation of metallic Ni crystallites. No diffraction peaks related to secondary phases (such as Ni_2Si) were detected, confirming that the ceramers are single-phase, and revealing the efficiency for generating in-situ metallic particles. The pyrolytic conversion of metal-containing polysiloxanes under an inert atmosphere is found to lead to an in-situ reduction of the metal precursor to metal nanoparticles, since hydrocarbons and hydrogen released during pyrolysis constitute a

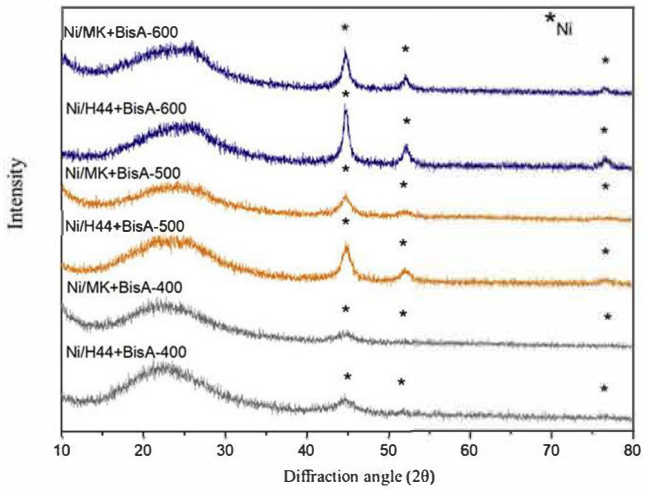

Fig. 6. XRD patterns of the Ni-containing ceramers pyrolyzed at 400, 500 and 600 °C.

reductive atmosphere [45]. By increasing the temperature, the intensity of the Ni peaks increases and the width decreases, which is associated with an increase in the crystallite size as seen in Table 2, indicating a remarkable enhance of nearly 60% in crystallite size at higher temperatures. The smallest crystallites were found for the samples pyrolyzed at 400 °C with 4.9 and 4.3 nm for Ni/H44 + BisA and Ni/Mk + BisA, respectively. With increasing pyrolysis temperature to 600 °C, the crystallite sizes increased to 13.5 and 11.5 nm, respectively. These results are in agreement with the TEM images presented in Fig. 5. The crystallite size calculated for ceramers pyrolyzed at 400 °C is almost the same as the particle size calculated from TEM, indicating the formation of single crystallite Ni particles. However, the crystallite size for ceramers pyrolyzed at 600 °C differs from TEM data, possibly due to the formation of Ni agglomerates consisting of several Ni crystallites.

Thus, these results demonstrate that Ni nanoparticles can be generated in-situ during pyrolysis with a homogeneous dispersion by using a complexing precursor. Moreover, the size of the particles is affected by increasing the temperature of pyrolysis for ceramers prepared either with H44 and MK polysiloxanes.

3.5. Catalytic activity

CO_2 methanation measurements were performed in order to analyze the applicability of the Ni-containing ceramers for catalytic purposes, considering the influence of the polysiloxane composition and the pyrolysis temperature on the catalytic activity. According to the characterization results, the ceramer's properties are influenced by the polysiloxane composition, and further, strongly depend on the pyrolysis temperature. Therefore, different behaviors and catalytic performances are expected. The CO_2 conversion and CH_4 selectivity of the ceramers are shown as a function of temperature (200–400 °C) in Fig. 7, along with results for the standard catalyst Ni/SiO_2-400.

It is clearly observed that CO_2 conversion and CH_4 selectivity increase with increasing the temperature, reaching the maximum rate at a reaction temperature of 400 °C. The highest conversion (~52%) and selectivity (~77%) can be observed for the ceramers pyrolyzed at 400 °C. On the other hand, ceramers pyrolyzed at 600 °C presented the lowest activity, with a decrease of around 20% and 50% in conversion and selectivity, respectively. Intermediate performances, however, were found for ceramers pyrolyzed at medium temperatures (500 °C). The explanation for this behavior is ascribed, mainly, to the Ni particle size and dispersion. Due to the structure-sensitivity of the reaction, the metal particle size greatly influences the catalytic performance, in which an improved performance is achieved with an optimum particle size [63,64]. According to the XRD and TEM results, smaller (~4 nm) and better dispersed Ni particles were found for ceramers pyrolyzed at 400 °C, thus, justifying the highest conversion and selectivity, once smaller particles offer a large number of surface atoms [65]. At higher pyrolysis temperatures (600 °C) larger particles were formed (~7 nm), leading to a lower metal surface, possibly explaining the lower conversion and selectivity levels.

Analyzing the ceramers pyrolyzed at the same temperature, a clear trend becomes obvious, characterized by the higher CO_2 conversion and CH_4 selectivity found for ceramers prepared from methyl polysiloxane (MK). For example, by comparing the ceramers pyrolyzed at 600 °C at a reaction temperature of 300 °C, Ni/MK + BisA exhibits 10% higher conversion and 18% higher selectivity than Ni/H44 + BisA. The same trend is found for ceramers pyrolyzed at 400 and 500 °C. When analyzing the characteristics of such ceramers, similar Ni particle size (see Table 2) and comparable surface areas (see Fig. 3) are found at each pyrolysis temperature. One first explanation for the better results of the MK-based ceramers is attributed to the larger pore sizes and pore volumes of these materials, which possibly improved the nickel particles accessibility, resulting in a higher catalytic performance. Moreover, the surface hydrophilicity plays a crucial role in the catalytic activity. It is known that water produced during the reaction has an inhibiting effect on the methanation activity, hindering the accessibility of the active sites and, thus, decreasing the reaction rate and selectivity [33]. By using a catalyst with a less hydrophilic surface this effect can be repressed and the amount of blocked active sites can be reduced. Hence, the more hydrophobic MK-based ceramers show a better catalytic activity and selectivity. The organic groups present in the polysiloxane precursors favor the hydrophobicity of the ceramers, therefore, since the phenyl groups in H44 are more easily decomposed then the methyl groups, more hydrophilic surfaces are obtained.

Therefore, the order of activity and selectivity for CO_2 methanation can be assigned as Ni/MK + BisA-400 > Ni/H44 + BisA-400 > Ni/MK + BisA-500 > Ni/H44 + BisA-500 > Ni/MK + BisA-600 > Ni/H44 + BisA-600. This behavior was also verified by Schubert et al. when testing Ni and Co-containing ceramers for CO_2 methanation and Fisher-Tropsch reactions, respectively [22]. By using APTES (3-aminopropyltriethoxysilane) as a complexing agent, microporous ceramers with high SSA (430–500 $m^2 g^{-1}$) and nanoparticles in the range of ~3 nm (Ni) and 5–10 nm (Co) were obtained. For the Ni-containing ceramers, the difference in catalytic activity was related to the different surface hydrophilicity. The highest activity was found for the catalysts with the lowest tendency to adsorb water, i.e. the ceramers pyrolyzed at 400 °C.

In order to compare the performance of the ceramers with those of existing catalysts, a standard catalyst Ni/SiO_2-400 was prepared and analyzed. Hence, it was possible to properly compare both materials under the same reaction conditions. With respect to the Ni/SiO_2-400 standard catalyst, the same dependency on the reaction temperature is observed, with maximum conversion and selectivity at 400 °C. The CO_2 conversion is low up to 300 °C, whereas from 350 °C on, an increase is observed, revealing better activity than ceramers pyrolyzed at 600 °C, however, lower than ceramers pyrolyzed at 400 and 500 °C. In relation to the selectivity, Ni/SiO_2-400 showed comparable performance to the ceramers pyrolyzed at 500 °C and improved selectivity than ceramers pyrolyzed at 600 °C. Although, selectivity up to 18% lower than ceramers pyrolyzed at 400 °C was obtained. This behavior may be intrinsically related to the accessibility and size of Ni particles as well as to the surface properties. Despite the fact of showing a hydrophilic surface and agglomerated Ni particles of about 8 nm (see supplementary data, Figs. S4 – S6), the impregnation method used to prepare the standard catalyst produces Ni enrichment on the surface of the support [66], which possibly favors the performance, leading to better results than ceramers pyrolyzed at 600 °C. However, the more hydrophobic surface of ceramers pyrolyzed at 400 °C associated with well-distributed and smaller Ni particles (4 nm), led to an improved performance due to the structure-sensitivity of the CO_2 methanation.

Ni catalyst can deactivate even at low temperatures due to sintering of Ni particles or carbon deposition, affecting its performance and

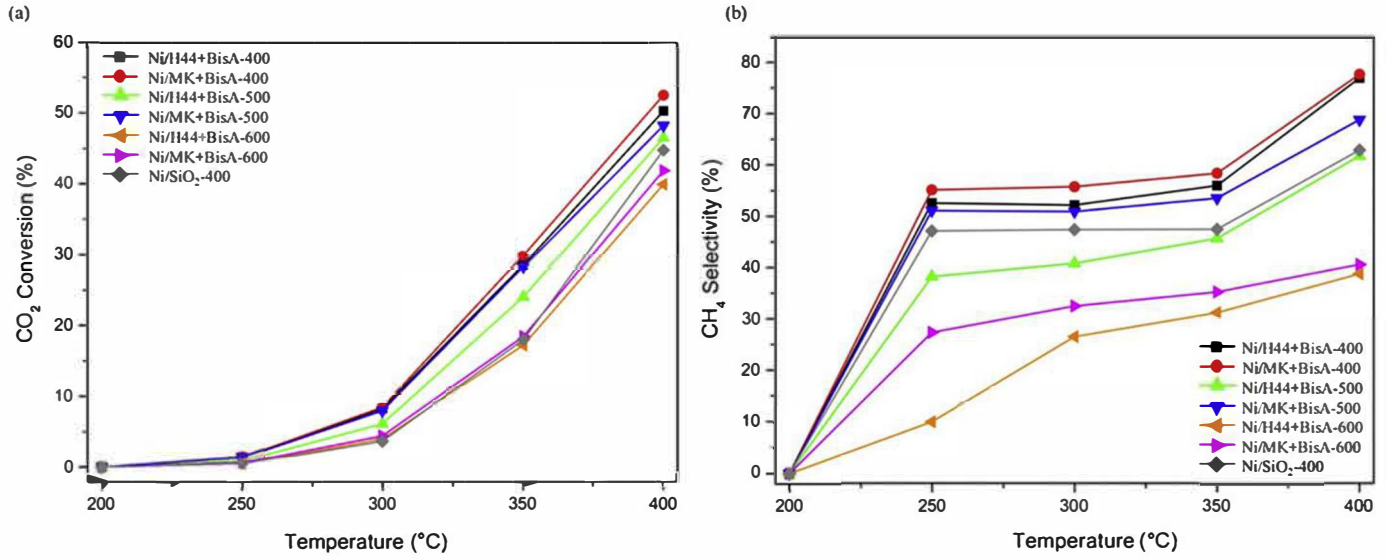

Fig. 7. (a) CO_2 conversion and (b) CH_4 selectivity for Ni-containing ceramers pyrolyzed at 400, 500 and 600 °C and Ni/SiO_2 pyrolyzed at 400 °C.

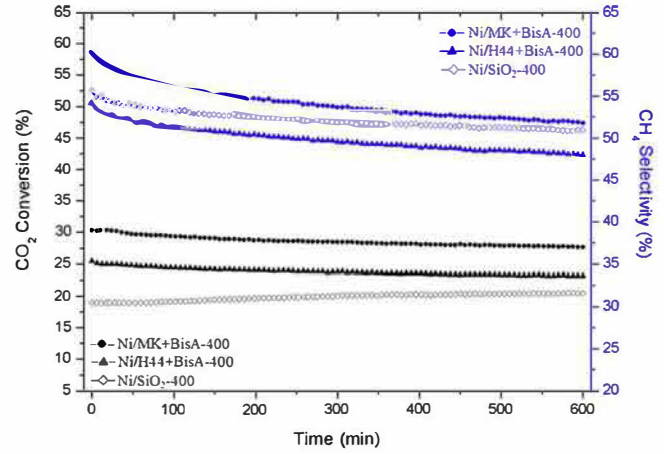

Fig. 8. CO_2 conversion (black) and CH_4 selectivity (blue) of catalysts at 350 °C for10 h. (For interpretation of the references to colour in this figure legend, the reader is referred to the Web version of this article.)

stability [67]. Therefore, in order to investigate the stability during the methanation reaction, catalysts pyrolyzed at 400 °C (Ni/H44 + BisA-400, Ni/MK + BisA-400 and Ni/SiO_2-400) were tested at 350 °C for 10 h as depicted in Fig. 8. The catalysts exhibited performance fairly close to the measurements in Fig. 7, indicating a good reproducibility within the experimental error. The standard catalyst showed continued conversion and selectivity, revealing a good stability of its Ni particles. In the same way, virtually constant conversion and selectivity during the entire test were displayed by the ceramers. The long-term performance of ceramers can be related to the improved dispersion of Ni particles and better particle-matrix interactions. As shown by the TEM images (Fig. 5(c) and 5(f)) after the 10 h test, no sintering of the Ni particles was observed, indicating their good stability.

In sum, these results demonstrate that the catalytic activity is influenced by the polysiloxane composition, pyrolysis temperature, and also by the reaction temperature. The CO_2 conversion and selectivity to CH_4 increase by decreasing pyrolysis temperature from 600 to 400 °C. Hydrophobic ceramers with small and well-dispersed Ni particles are more suitable for CO_2 methanation, showing good stability and improved conversion and selectivity when compared to a standard catalyst. A further optimization of the ceramers based e.g. on the formation of smaller and well-distributed Ni particles is expected to further improve the catalytic activity.

3.6. *In-situ analysis*

In-situ diffraction analysis was conducted during a simulated methanation reaction in order to verify possible phase changes and the evolution of the Ni crystallite sizes through the catalytic test. This investigation allows a better understanding on the stability of the metal particle during the reaction. The test was conducted by reproducing during a shorter time the same conditions of the catalytic test. Fig. 9(a–d) shows the in-situ XRD patterns of the ceramers pyrolyzed at 400 and 600 °C during the first hour of CO_2 methanation reaction.

The diffraction peaks of Ni are shifted to higher angles located at approximately 51 and 60° 2θ, once a radiation with a higher wavelength of 1.7712 Å was applied in the diffractometer. The peaks did not suffer considerable changes and no undesired phase formation was identified during the reaction time, demonstrating that the structure is preserved. The influence of the pyrolysis temperature is clearly observed for both types of ceramer. At pyrolysis temperature of 600 °C (Fig. 9 (c,d)), the peaks are found to be more intense and the width narrower, indicating the presence of bigger particles and/or the formation of agglomerates, in accordance with the XRD patterns in Fig. 6.

The utmost interesting aspect observed from the in-situ XRD experiments is the stability of the Ni crystallites during the reaction as depicted in Fig. 9(e), indicating no further growth during the test, corroborating with the TEM analysis of the spent ceramers. For both H44 and MK-based ceramers at 400 and 600 °C, the crystallite sizes of Ni are maintained constant. At 400 °C both ceramers present similar crystallite sizes (5.8 nm), whereas at 600 °C Ni/MK + BisA-600 shows smaller crystallites (~10.8 nm) compared to Ni/H44 + BisA-600 (~13.3 nm). These results are in good agreement with the diffraction data presented early (see Table 2). A small difference in crystallite sizes comparing both XRD and in-situ XRD is to be expected once different devices were used to measure the samples.

Accordingly, these results demonstrate that the structure and crystallite size of Ni are stable during the catalytic reaction, indicating no sintering effects.

In summary, the noted advantage is the possibility to obtain a material with easily adjustable properties and enhanced catalytic performance from a polymer-derived ceramic. Using a simple processing methodology, materials with tailorable hydrophilicity, hierarchical porosity and high surface area containing nanodispersed metal particles could be generated. Therefore, metal-containing ceramers are promising materials to be applied in catalytic applications.

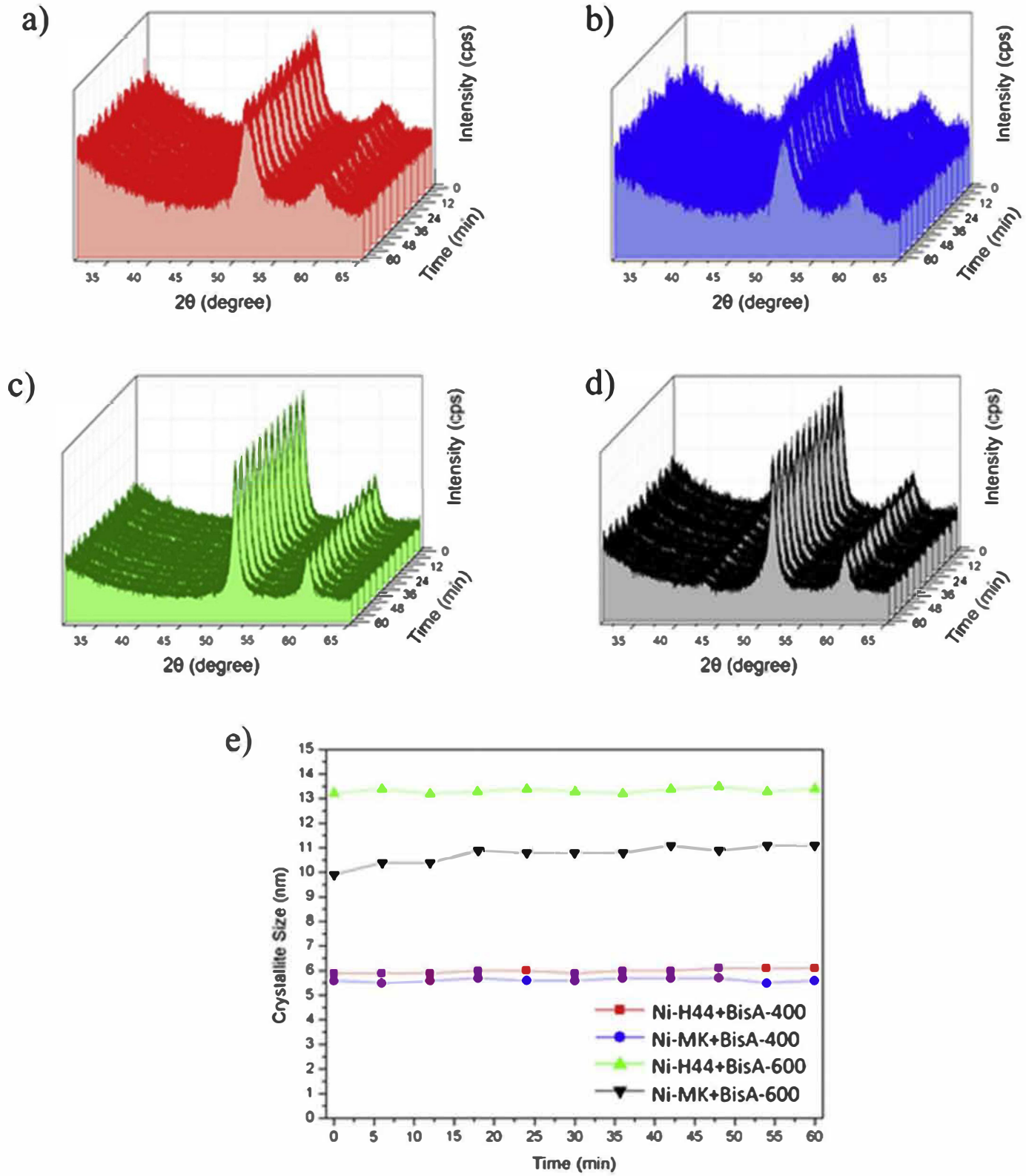

Fig. 9. In-situ XRD patterns during a simulated CO_2 methanation reaction for (a) Ni-H44 + BisA-400, (b) Ni-MK + BisA-400, (c) Ni-H44 + BisA-600 and (d) Ni-MK + BisA-600 ceramers; and (e) crystallite size versus time on stream.

4. Conclusions

In this work, Ni-containing hybrid ceramics were prepared by a simple route using commercially available and low-cost polysiloxanes under low pyrolysis temperatures. The PDC route is an advantageous and promising methodology to easily prepare catalysts with adjustable and improved characteristics. Polysiloxanes with either methyl or methylphenyl groups were used in order to evaluate the influence of the precursor composition as well as the pyrolysis temperature (400–600 °C) on the ceramers properties and catalytic activity toward CO_2 methanation.

The pyrolysis temperature revealed to be the main factor for tailoring the ceramers properties. The pyrolytic conversion of polysiloxanes combined with BisA at different pyrolysis temperature generated porous materials with hierarchical porosity (micro-, meso- and macroporosity) and high specific surface areas (100–550 $m^2 g^{-1}$), providing a good accessibility of the catalyst particles and facilitating the internal mass transfer. Moreover, hydrophobic or hydrophilic surfaces were generated and metallic Ni particles obtained in-situ during decomposition. Due to the use of BisA as complexing siloxane, Ni particles were homogeneously distributed, showing average sizes of 4–7 nm. Their stable embedding avoided sintering of the particles even during long hours of reaction. The surface hydrophilicity and Ni particle size could be altered by decreasing pyrolysis temperature, and thus, increasing the performance of the catalysts.

In terms of catalytic properties, CO_2 conversion and CH_4 selectivity could be improved by increasing the reaction temperature and decreasing the pyrolysis temperature of ceramers. Therefore, the ceramers pyrolyzed at 400 °C exhibited the highest CO_2 conversion with selectivity up to ~77% and an overall good stability during 10 h of reaction. For structure-sensitive reactions as e.g. CO_2 methanation, the catalytic performance is closely related to the intrinsic properties of the catalyst, including the size of metal particles and hydrophilicity. A less hydrophilic surface and smaller Ni particles showed a positive effect on the stability and activity. In contrast, bigger Ni particles and more hydrophilic surfaces led to a significantly lower conversion and selectivity. Ceramers prepared using MK as polysiloxane precursor showed a more hydrophobic surface, due to the better thermal resistance of the methyl groups, and thus, improved catalytic activity since water presents an inhibiting effect during the methanation reaction.

In summary, it could be demonstrated that metal-containing ceramers are promising materials for catalytic applications at low-temperature reactions and for long periods, presenting improved and long-term activity, stable performance and sintering resistance, owing to their enhanced and tailorable properties.

Acknowledgments

This work was supported by the Brazilian Federal Agency for the Improvement of Higher Education Personnel (CAPES) and by the German Research Foundation (DFG) within the Research Training Group GRK 1860 "Micro-, meso- and macroporous nonmetallic Materials: Fundamentals and Applications" (MIMENIMA). The authors thank the Brazilian Synchrotron Light Laboratory (LNLS) for the use of the D10B-XPD beamline to perform the in-situ X-ray diffraction experiments.

Appendix A. Supplementary data

Supplementary data to this article can be found online at https://doi.org/10.1016/j.micromeso.2018.11.006.

References

[1] E. Bernardo, L. Fiocco, G. Parcianello, E. Storti, P. Colombo, Advanced ceramics from preceramic polymers modified at the nano-scale: a review, Materials 7 (2014) 1927–1956.
[2] P. Colombo, G. Mera, R. Riedel, G.D. Sorarù, Polymer-derived ceramics: 40 years of research and innovation in advanced ceramics, J. Am. Ceram. Soc. 93 (2010) 1805–1837.
[3] B.V.M. Kumar, K. Young-Wook, Processing of polysiloxane-derived porous ceramics: a review, Sci. Technol. Adv. Mater. 11 (2010) 044303.
[4] M. Wilhelm, C. Soltmann, D. Koch, G. Grathwohl, Ceramers—functional materials for adsorption techniques, J. Eur. Ceram. Soc. 25 (2005) 271–276.
[5] T. Prenzel, M. Wilhelm, K. Rezwan, Pyrolyzed polysiloxane membranes with tailorable hydrophobicity, porosity and high specific surface area, Microporous Mesoporous Mater. 169 (2013) 160–167.
[6] N. Li, Y. Cao, R. Zhao, Y. Xu, L. An, Polymer-derived SiAlOC ceramic pressure sensor with potential for high-temperature application, Sensor Actuator Phys. 263 (2017) 174–178.
[7] A. Guo, M. Roso, M. Modesti, J. Liu, P. Colombo, Hierarchically structured polymer-derived ceramic fibers by electrospinning and catalyst-assisted pyrolysis, J. Eur. Ceram. Soc. 34 (2014) 549–554.
[8] M. Wilamowska, M. Graczyk-Zajac, R. Riedel, Composite materials based on polymer-derived SiCN ceramic and disordered hard carbons as anodes for lithium-ion batteries, J. Power Sources 244 (2013) 80–86.
[9] K. Wang, J. Unger, J.D. Torrey, B.D. Flinn, R.K. Bordia, Corrosion resistant polymer derived ceramic composite environmental barrier coatings, J. Eur. Ceram. Soc. 34 (2014) 3597–3606.
[10] F. Guo, D. Su, Y. Liu, J. Wang, X. Yan, J. Chen, S. Chen, High acid resistant SiOC ceramic membranes for wastewater treatment, Ceram. Int. 44 (11) (2018) 13444–13448.
[11] C. Vakifahmetoglu, E. Pippel, J. Woltersdorf, P. Colombo, Growth of one-dimensional nanostructures in porous polymer-derived ceramics by catalyst-assisted pyrolysis. Part I: iron catalyst, J. Am. Ceram. Soc. 93 (2010) 959–968.
[12] C. Vakifahmetoglu, P. Colombo, S.M. Carturan, E. Pippel, J. Woltersdorf, Growth of one-dimensional nanostructures in porous polymer-derived ceramics by catalyst-assisted pyrolysis. Part II: cobalt catalyst, J. Am. Ceram. Soc. 93 (2010) 3709–3719.
[13] M. Zaheer, G. Motz, R. Kempe, The generation of palladium silicide nanoalloy particles in a SiCN matrix and their catalytic applications, J. Mater. Chem. 21 (2011) 18825.
[14] M. Zaheer, J. Hermannsdörfer, W.P. Kretschmer, G. Motz, R. Kempe, Robust heterogeneous nickel catalysts with tailored porosity for the selective hydrogenolysis of aryl ethers, ChemCatChem 6 (2014) 91–95.
[15] M. Zaheer, C.D. Keenan, J. Hermannsdörfer, E. Roessler, G. Motz, J. Senker, R. Kempe, Robust microporous monoliths with integrated catalytically active metal sites investigated by hyperpolarized 129Xe NMR, Chem. Mater. 24 (2012) 3952–3963.
[16] E. Kockrick, R. Frind, M. Rose, U. Petasch, W. Böhlmann, D. Geiger, M. Herrmann, S. Kaskel, Platinum induced crosslinking of polycarbosilanes for the formation of highly porous CeO_2/silicon oxycarbide catalysts, J. Mater. Chem. 19 (2009) 1543.
[17] M. Wójcik-Bania, A. Krowiak, J. Strzezik, M. Hasik, Pt supported on cross-linked poly(vinylsiloxanes) and SiCO ceramics — new materials for catalytic applications, Mater. Des. 96 (2016) 171–179.
[18] M. Adam, S. Kocanis, T. Fey, M. Wilhelm, G. Grathwohl, Hierarchically ordered foams derived from polysiloxanes with catalytically active coatings, J. Eur. Ceram. Soc. 34 (2014) 1715–1725.
[19] M. Adam, M. Bäumer, M. Schowalter, J. Birkenstock, M. Wilhelm, G. Grathwohl, Generation of Pt- and Pt/Zn-containing ceramers and their structuring as macro/microporous foams, Chem. Eng. J. 247 (2014) 205–215.
[20] M. Wilhelm, M. Adam, M. Bäumer, G. Grathwohl, Synthesis and properties of porous hybrid materials containing metallic nanoparticles, Adv. Eng. Mater. 10 (2008) 241–245.
[21] M. Adam, M. Wilhelm, G. Grathwohl, Polysiloxane derived hybrid ceramics with nanodispersed Pt, Microporous Mesoporous Mater. 151 (2012) 195–200.
[22] M. Schubert, M. Wilhelm, S. Bragulla, C. Sun, S. Neumann, T.M. Gesing, P. Pfeifer, K. Rezwan, M. Bäumer, The influence of the pyrolysis temperature on the material properties of cobalt and nickel containing precursor derived ceramics and their catalytic use for CO_2 methanation and Fischer–Tropsch synthesis, Catal. Lett. 147 (2016) 472–482.
[23] S. Saeidi, N.A.S. Amin, M.R. Rahimpour, Hydrogenation of CO_2 to value-added products—a review and potential future developments, J. CO_2 Util. 5 (2014) 66–81.
[24] J. Gao, Q. Liu, F. Gu, B. Liu, Z. Zhong, F. Su, Recent advances in methanation catalysts for the production of synthetic natural gas, RSC Adv. 5 (2015) 22759–22776.
[25] P. Panagiotopoulou, D.I. Kondarides, X.E. Verykios, Selective methanation of CO over supported noble metal catalysts: effects of the nature of the metallic phase on catalytic performance, Appl. Catal. Gen. 344 (2008) 45–54.
[26] M.R. Gogate, R.J. Davis, Comparative study of CO and CO_2 hydrogenation over supported Rh–Fe catalysts, Catal. Commun. 11 (2010) 901–906.
[27] K.P. De Jong, J.H.E. Glezer, H.P.C.E. Kuipers, A. Knoester, C.A. Emeis, Highly dispersed Rh/SiO_2 and Rh/MnO/SiO_2 catalysts: 1. Synthesis, characterization, and CO hydrogenation activity, J. Catal. 124 (1990) 520–529.
[28] G.D. Weatherbee, C.H. Bartholomew, Hydrogenation of CO_2 on group VIII metals: I. Specific activity of $NiSiO_2$, J. Catal. 68 (1981) 67–76.
[29] G.D. Weatherbee, C.H. Bartholomew, Hydrogenation of CO_2 on group VIII metals: IV. Specific activities and selectivities of silica-supported Co, Fe, and Ru, J. Catal. 87 (1984) 352–362.
[30] F.-W. Chang, T.-J. Hsiao, S.-W. Chung, J.-J. Lo, Nickel supported on rice husk ash — activity and selectivity in CO_2 methanation, Appl. Catal. Gen. 164 (1997) 225–236.
[31] H. Muroyama, Y. Tsuda, T. Asakoshi, H. Masitah, T. Okanishi, T. Matsui, K. Eguchi, Carbon dioxide methanation over Ni catalysts supported on various metal oxides, J. Catal. 343 (2016) 178–184.
[32] T.A. Le, M.S. Kim, S.H. Lee, T.W. Kim, E.D. Park, CO and CO_2 methanation over supported Ni catalysts, Catal. Today 293–294 (2017) 89–96.
[33] M.A.A. Aziz, A.A. Jalil, S. Triwahyono, M.W.A. Saad, CO_2 methanation over Ni-promoted mesostructured silica nanoparticles: influence of Ni loading and water vapor on activity and response surface methodology studies, Chem. Eng. J. 260 (2015) 757–764.
[34] Y. Yan, Y. Dai, Y. Yang, A.A. Lapkin, Improved stability of Y_2O_3 supported Ni catalysts for CO_2 methanation by precursor-determined metal-support interaction, Appl. Catal. B Environ. 237 (2018) 504–512.
[35] W. Wang, S. Wang, X. Ma, J. Gong, Recent advances in catalytic hydrogenation of carbon dioxide, Chem. Soc. Rev. 40 (2011) 3703–3727.
[36] C.K. Vance, C.H. Bartholomew, Hydrogenation of carbon dioxide on group VIII metals: III, Effects of support on activity/selectivity and adsorption properties of nickel, Appl. Catal. 7 (1983) 169–177.
[37] J.-N. Park, E.W. McFarland, A highly dispersed Pd–Mg/SiO_2 catalyst active for

methanation of CO_2, J. Catal. 266 (2009) 92–97.
[38] W.-J. Wang, Y.-W. Chen, Influence of metal loading on the reducibility and hydrogenation activity of cobalt/alumina catalysts, Appl. Catal. 77 (1991) 223–233.
[39] A.A. Lemonidou, M.A. Goula, I.A. Vasalos, Carbon dioxide reforming of methane over 5wt.% nickel calcium aluminate catalysts – effect of preparation method, Catal. Today 46 (1998) 175–183.
[40] X. Yan, Y. Liu, B. Zhao, Z. Wang, Y. Wang, C.-j. Liu, Methanation over Ni/SiO_2: effect of the catalyst preparation methodologies, Int. J. Hydrogen Energy 38 (2013) 2283–2291.
[41] Q. Liu, Y. Tian, One-pot synthesis of NiO/SBA-15 monolith catalyst with a three-dimensional framework for CO_2 methanation, Int. J. Hydrogen Energy 42 (2017) 12295–12300.
[42] Y.-H. Huang, J.-J. Wang, Z.-M. Liu, G.-D. Lin, H.-B. Zhang, Highly efficient Ni-ZrO_2 catalyst doped with Yb_2O_3 for co-methanation of CO and CO_2, Appl. Catal. Gen. 466 (2013) 300–306.
[43] S. Hwang, J. Lee, U.G. Hong, J.G. Seo, J.C. Jung, D.J. Koh, H. Lim, C. Byun, I.K. Song, Methane production from carbon monoxide and hydrogen over nickel–alumina xerogel catalyst: effect of nickel content, J. Ind. Eng. Chem. 17 (2011) 154–157.
[44] A. Zhao, W. Ying, H. Zhang, H. Ma, D. Fang, Ni–Al_2O_3 catalysts prepared by solution combustion method for syngas methanation, Catal. Commun. 17 (2012) 34–38.
[45] T. Schmalz, T. Kraus, M. Günthner, C. Liebscher, U. Glatzel, R. Kempe, G. Motz, Catalytic formation of carbon phases in metal modified, porous polymer derived SiCN ceramics, Carbon 49 (2011) 3065–3072.
[46] B.D. Cullity, S.R. Stock, Elements of X-Ray Diffraction, third ed., Pearson Education Limited, 2014.
[47] J.D. Jovanovic, M.N. Govedarica, P.R. Dvornic, I.G. Popovic, The thermogravimetric analysis of some polysiloxanes, Polym. Degrad. Stabil. 61 (1998) 87–93.
[48] C. Vakifahmetoglu, P. Colombo, A direct method for the fabrication of macroporous SiOC ceramics from preceramic polymers, Adv. Eng. Mater. 10 (2008) 256–259.
[49] M. Scheffler, T. Gambaryan-Roisman, T. Takahashi, J. Kaschta, H. Muenstedt, P. Buhler, P. Greil, Pyrolytic Decomposition of Preceramic Organo Polysiloxanes, (2000).
[50] F.I. Hurwitz, P. Heimann, S.C. Farmer, D.M. Hembree, Characterization of the pyrolytic conversion of polysilsesquioxanes to silicon oxycarbides, J. Mater. Sci. 28 (1993) 6622–6630.
[51] International union of pure and applied chemistry, reporting physisorption data for gas/solid systems with special rederence to the determinantion of surface area and porosity, Pure Appl. Chem. 57 (1985) 603–619.
[52] T. Prenzel, T.L.M. Guedes, F. Schlüter, M. Wilhelm, K. Rezwan, Tailoring surfaces of hybrid ceramics for gas adsorption – from alkanes to CO_2, Separ. Purif. Technol. 129 (2014) 80–89.
[53] T. Prenzel, M. Wilhelm, K. Rezwan, Tailoring amine functionalized hybrid ceramics to control CO_2 adsorption, Chem. Eng. J. 235 (2014) 198–206.
[54] M. Adam, C. Vakifahmetoglu, P. Colombo, M. Wilhelm, G. Grathwohl, G. Soraru, Polysiloxane-derived ceramics containing nanowires with catalytically active tips, J. Am. Ceram. Soc. 97 (2014) 959–966.
[55] C. Vakifahmetoglu, D. Zeydanli, P. Colombo, Porous polymer derived ceramics, Mater. Sci. Eng. R Rep. 106 (2016) 1–30.
[56] P. Colombo, Engineering porosity in polymer-derived ceramics, J. Eur. Ceram. Soc. 28 (2008) 1389–1395.
[57] S. Harald, K. Dietmar, G. Georg, C. Paolo, Micro-/Macroporous ceramics from preceramic precursors, J. Am. Ceram. Soc. 84 (2001) 2252–2255.
[58] X. Bai, S. Wang, T. Sun, S. Wang, The sintering of Ni/Al_2O_3 methanation catalyst for substitute natural gas production, React. Kinet. Mech. Catal. 112 (2014) 437–451.
[59] M.S. Kamal, S.A. Razzak, M.M. Hossain, Catalytic oxidation of volatile organic compounds (VOCs) – a review, Atmos. Environ. 140 (2016) 117–134.
[60] F. Pinna, Supported metal catalysts preparation, Catal. Today 41 (1998) 129–137.
[61] C. Harms, M. Adam, K.A. Soliman, M. Wilhelm, L.A. Kibler, T. Jacob, G. Grathwohl, New electrocatalysts with pyrolyzed siloxane matrix, Electrocatalysis 5 (2014) 301–309.
[62] M. Scheffler, P. Greil, A. Berger, E. Pippel, J. Woltersdorf, Nickel-catalyzed in situ formation of carbon nanotubes and turbostratic carbon in polymer-derived ceramics, Mater. Chem. Phys. 84 (2004) 131–139.
[63] C. Vogt, E. Groeneveld, G. Kamsma, M. Nachtegaal, L. Lu, C.J. Kiely, P.H. Berben, F. Meirer, B.M. Weckhuysen, Unravelling structure sensitivity in CO_2 hydrogenation over nickel, Nature Catalysis 1 (2018) 127–134.
[64] J.K. Kesavan, I. Luisetto, S. Tuti, C. Meneghini, G. Iucci, C. Battocchio, S. Mobilio, S. Casciardi, R. Sisto, Nickel supported on YSZ: the effect of Ni particle size on the catalytic activity for CO_2 methanation, J. CO_2 Util. 23 (2018) 200–211.
[65] N. Toshima, Metal nanoparticles for catalysis, in: L.M. Liz-Marzán, P.V. Kamat (Eds.), Nanoscale Materials, Springer US, Boston, MA, 2003, pp. 79–96.
[66] W. Cai, Q. Zhong, Y. Zhao, Fractional-hydrolysis-driven formation of non-uniform dopant concentration catalyst nanoparticles of Ni/$Ce_xZr_{1-x}O_2$ and its catalysis in methanation of CO_2, Catal. Commun. 39 (2013) 30–34.
[67] C.H. Bartholomew, Mechanisms of catalyst deactivation, Appl. Catal. Gen. 212 (2001) 17–60.